EXPERIMENTAL STUDY FOR WIND ENERGY HARVESTING BASED ON THE AEROELASTIC EXCITATION OF A SEMI-CIRCULAR CYLINDER

MARINA G. LÓPEZ-ARIAS, FELIX NIETO & SANTIAGO HERNÁNDEZ
School of Civil Engineering, University of La Coruna, Spain

ABSTRACT

In this study a semi-circular cylinder at a wind incidence angle of 0° (rectilinear side parallel to the flow) has been adopted as a wind-excited bluff body for low-scale energy generation. This geometry has shown vortex-induced vibration (VIV) at low wind speeds and galloping excitation for higher values inside the studied range. The preliminary results of a wind tunnel campaign conducted using a sectional model of a semi-circular cylinder are reported and both VIV and galloping phenomena were identified, along with a relatively infrequent VIV-galloping interference case for the torsional degree of freedom. Based on these results, a prototype of an energy harvester has been designed and constructed. This prototype has also been studied by means of wind tunnel tests, obtaining the voltage output and the average power output for different wind speeds. Both VIV and galloping excitation were identified, finding that the power generation is larger for higher wind reduced speeds, as the prototype experiences galloping. For the prototype at 0° angle of attack, nondimensional amplitudes of oscillation up to 0.3 were measured, while the averaged power output reached 1700 µW. This work has signalled additional issues to consider for a throughout characterization of the harvester such as turbulent incoming flow or different angle of attack between the wind and the bluff body.
Keywords: energy harvesting, piezoelectricity, vortex-induced vibration, galloping, semi-circular cylinder, wind tunnel.

1 INTRODUCTION

There is, nowadays, a general consensus about the negative impact caused by the environmental degradation of our planet and the risks posed by climate change. Consequently, there is a growing pressure to develop resource-efficient energy generation systems. Policy bodies are implementing several actions aiming at setting ambitious goals for making even more sustainable our economy. Examples of this are the European Green Deal, headed by the European Commission and the Millennium Development Goals, sponsored by the United Nations.

Energy harvesting technologies may help in achieving sustainability goals. According to Elvin and Erturk [1], energy harvesters transform mechanical energy into electrical power by using piezoelectric, electromagnetic, electrostatic, magnetostrictive or magnetoelectric conversion methods. Piezoelectric energy harvesting is the most widely used method due to its ease of application, relatively high voltage output, and mature fabrication methods. The piezoelectric effect appears due to the symmetric configuration of the crystalline structure of the materials showing this property. When the stress in the material is null, no polarization of the ions takes place; however, when the crystal is under stress, its cubic structure shows a relative shift of the cations located at the body's centre, resulting in a polarization of the atom that gives place to an electrical field in the piezoelectric material.

From an environmentally sustainable perspective, the use of renewable source for generating the mechanical energy in the harvester is of utmost importance. Because of this, wind-induced oscillations are studied aiming at enhancing their effects to obtain a relatively large mechanical energy that can be transformed into electrical power. Consequently, bluff

bodies that are known to be sensitive to aeroelastic effects are used to generate large oscillations in the harvester at relatively low wind speeds.

The objective of this work is to assess the feasibility of a semi-circular cylinder, whose aerodynamic characteristics were previously studied based on experimental tests and numerical simulations [2], to generate large wind-induced oscillations in a classical harvester configuration based on a cantilever beam with the bluff body attached to its tip and a sheet of piezoelectric material bounded close to the fixed end. Other alternative geometries have been studied as tip bluff bodies [3], [4], also considering modifications in the reference shape. However, semi-circular cylinders at 0° angle of attack have not been previously addressed, to the authors' knowledge.

The basic aeroelastic phenomena are introduced in Section 2. Then, the preliminary sectional model tests are reported in Section 3. Based on the data obtained, a relatively large-scale prototype is designed, which is reported in Section 4. In Section 5, the outcome of the wind tunnel campaign of the prototype is provided, and the concluding remarks are summarized in Section 6.

2 AEROELASTIC PHENOMENA

There is a wide range of aeroelastic phenomena that may take place when the flow interacts with a bluff cylinder. The basic ones are vortex-induced vibration, galloping and flutter. Vortex-induced vibration (VIV), is caused by the oscillations induced by the fluctuating pressures acting on the elastic structure [5]. Galloping is due to the vibrations arising from fluid forces induced by structural vibration; as the structure oscillates, its orientation changes and fluid-induced force oscillates [5]. Usually, flutter is used to designate the coupled heave–pitch instability due to the vortices shed from the trailing edge of the elastic body causing a phase shift of the fluid loading relative to the body motion [6]. It should be noticed that according to [5], the differences between flutter and galloping are mainly related with the historical usage of these terms.

The main aerodynamic parameters used to characterize the response of the semi-circular cylinders are introduced next.

Drag, lift and moment coefficients (C_D, C_L, C_M) provide a non-dimensional measure of the mean flow-induced loads acting on the static semi-circular cylinder per unit of length. The force and moment components are defined as

$$C_D = \frac{F_D}{\frac{1}{2}\rho U^2 A}; \quad C_L = \frac{F_L}{\frac{1}{2}\rho U^2 A}; \quad C_M = \frac{M}{\frac{1}{2}\rho U^2 BA}, \tag{1}$$

where F_D is the drag force acting on the body, F_L is the lift force and M is the moment. ρ is the fluid density, U the reference flow velocity, A is the reference area and B the reference dimension.

Vortex-induced vibrations appear when the frequency at which vortices are shed from the body is close to one of the natural frequencies of the dynamical system. The non-dimensional frequency at which vortices are shed from the static body is the so-called Strouhal number, being f the vortex-shedding frequency and D the across-wind reference dimension of the body

$$St = \frac{fD}{U}. \tag{2}$$

The dynamic equilibrium equation of a system excited by VIV can be expressed as

$$m\ddot{y}(t) + c\dot{y}(t) + ky(t) = F(\ddot{y}, \dot{y}, y, t), \tag{3}$$

where y represents the across-wind displacement of the body, m is the mass per unit length, c the mechanical damping, k the stiffness and F the fluid-induced force per span length.

Galloping is an aeroelastic instability caused by the negative aerodynamic damping introduced in the dynamical system. For the plunge degree of freedom, the dynamic equilibrium equation is the following

$$m(\ddot{y} + 2\zeta\omega_n\dot{y} + \omega_n^2 y) = -\frac{1}{2}\rho U^2 D\left(C_D + \frac{d(C_L)}{d\alpha}\right)\frac{\dot{y}}{U}. \tag{4}$$

In eqn (4), ζ is the mechanical damping ratio, ω_n is the natural circular frequency of oscillation and $d/d\alpha$ is the derivative with respect to the wind flow angle of attack α.

3 PRELIMINARY WIND TUNNEL TESTS

Aiming at characterising the aeroelastic behaviour of the semi-circular cylinder, a first round of sectional model wind tunnel tests was conducted. The goal of these tests was to identify the ranges of reduced velocities showing an apparent excitation of the model, which would be indicative of potential energy harvesting resources.

In Fig. 1, an image of the sectional model inside the test chamber is presented. The natural frequencies of the sectional model, which have been obtained by conducting free oscillation tests in still air, are reported in Table 1. The damping ratio relative to critical of the dynamical system was $\xi=0.0014$. Table 1 shows the proximity between the natural frequencies for the plunge and torsional degrees of freedom and the consequent potential for coupled galloping.
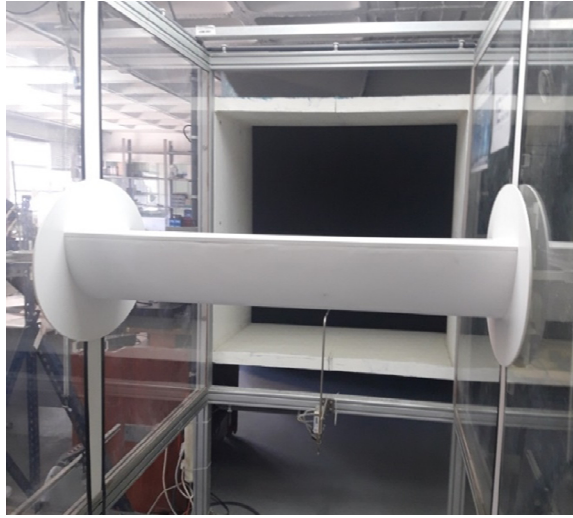

Figure 1:   Sectional model of the semi-circular cylinder mounted in the wind tunnel at 0° angle of attack.

Table 1: Natural frequencies of the sectional model.

Degree of freedom	Natural frequency (Hz)
Along-wind	3.52
Across-wind	1.56
Torsional	1.86

3.1 Aeroelastic response in the plunge degree of freedom

Free-to-oscillate wind tunnel tests have been conducted for the sectional model with the dynamic characteristics introduced above. The flow speed inside the test chamber has been increased gradually, and the plunge and torsional oscillations have been registered based on the loads acting on the springs supporting the sectional model. In Fig. 2, the non-dimensional steady amplitudes of oscillation obtained along the range of considered flow speeds (0 to 10 m/s) are reported. It can be identified a clear "bell" inside the interval between 1 m/s and 2 m/s, reaching a peak value for the non-dimensional amplitude of oscillation of 0.17. This is a typical VIV response. These tests have allowed to identify a region at relatively low reduced velocity ($U/(f_v D)$), being f_v the plunge natural frequency) showing wind-induced oscillation, and therefore potential for energy harvesting exploitation. It can also be noted how the steady oscillation in the plunge degree of freedom grows for flow speeds higher than 2 m/s, reaching amplitudes of oscillations larger than the VIV peak mentioned before. This behaviour will be further discussed in the next section, and it shows the ability to generate energy for values of the reduced velocity higher than 10.
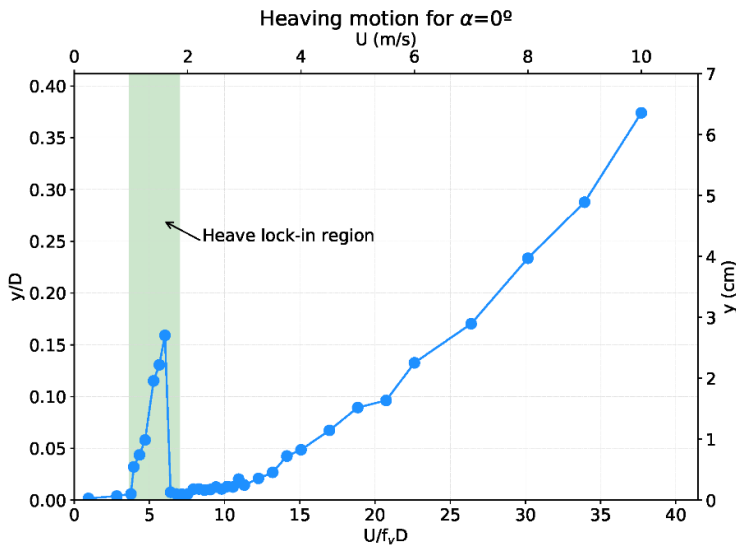

Figure 2: Experimental plunge amplitude–velocity curve for the semi-circular cylinder at 0° angle of attack.

3.2 Aeroelastic response in the torsional degree of freedom

The sectional model tested in the wind tunnel is a 3 degrees-of-freedom dynamical system, and in Fig. 3 the amplitudes of torsional oscillation obtained for different flow speeds are reported.

It can be also noted in Fig. 3, a bell in the range of wind speeds between 2 m/s and 3 m/s, characteristic of torsional VIV. However, the tail of the bell does not reach a null oscillation value, but increases again shortly after starting to decrease. This behaviour is typical of partial interference between VIV and galloping, as it has been described by Mannini et al. [7] for a 1.5 side ratio rectangular cylinder.
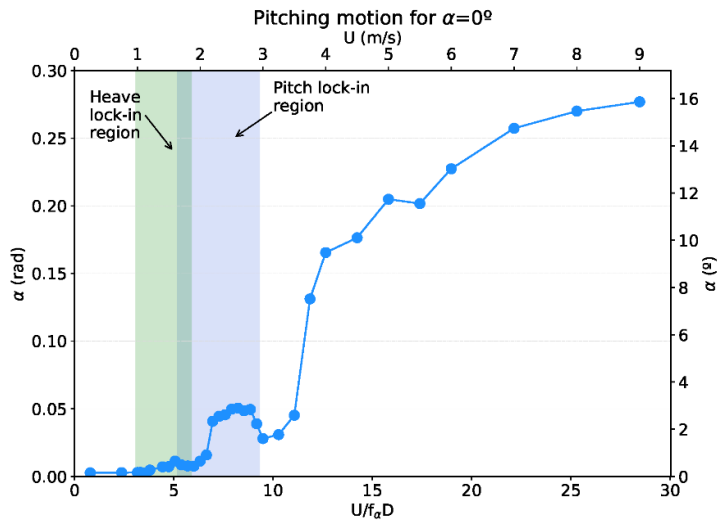
Pitching motion for $\alpha = 0^\circ$

Figure 3:   Experimental torsional amplitude–velocity curve for the semi-circular cylinder at 0° angle of attack.

As in the former case, the non-negligible amplitudes of oscillation in the torsional degree of freedom would point towards a potential energy generation capability.

3.3 Coupled plunge-torsional oscillations

In Table 1, the natural frequencies of the plunge and torsional degrees of freedom were reported, and it is clear their proximity, which could facilitate the coupling of these modes when they are excited by the wind action. Indeed, in the amplitude–velocity curves reported in Figs 2 and 3, it can be perused how the amplitude of oscillation grows in the two degrees of freedom for reduced velocities higher than 10. In order to better understand the aeroelastic response of the model, in Fig. 4 the evolution of the main plunge and torsional excitation frequencies with the flow speed is reported. In the chart, the lock-in regions obtained for the plunge and torsional VIV can be identified as plateaus of nearly constant frequency. Furthermore, for flow speeds higher than 4 m/s, both plunge and torsional frequencies of excitation coalescence to nearly the same values, indicating the coupled galloping excitation of the dynamical system.

4 ENERGY HARVESTER PROTOTYPE DESIGN

A prototype of an energy harvester based on cantilever beams whose deflection is induced by the wind-induced oscillation of a semi-circular cylinder located at the cantilevers' tips has been designed. Close to the fixed end of one of the cantilevers, a Macro-Fiber Composite (MFC) piezoelectric sheet is bonded, and it is used as a transducer to transform mechanical energy into electrical energy adopting the 31-mode arrangement. The manufacturer of the MFC sheet is Smart Material Corp. In Fig. 5(a) a scheme of the device is provided, including the main dimensions, since the goal has been to devise a prototype as large as possible, which could eventually represent a real scale device. In this manner, scale factors in the conversion process can be avoided. In Fig. 5(b) a photography of the prototype mounted in the test chamber is reported.
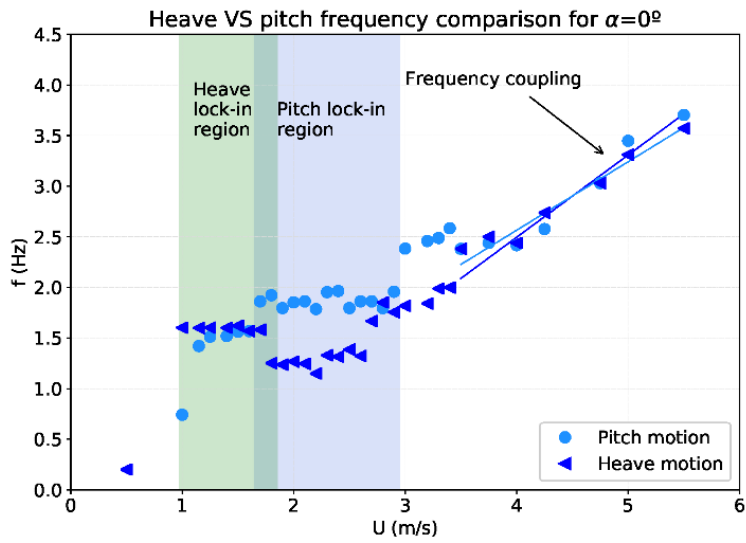
Figure 4: Plunge and torsional excitation frequencies vs flow speed at 0° angle of attack.
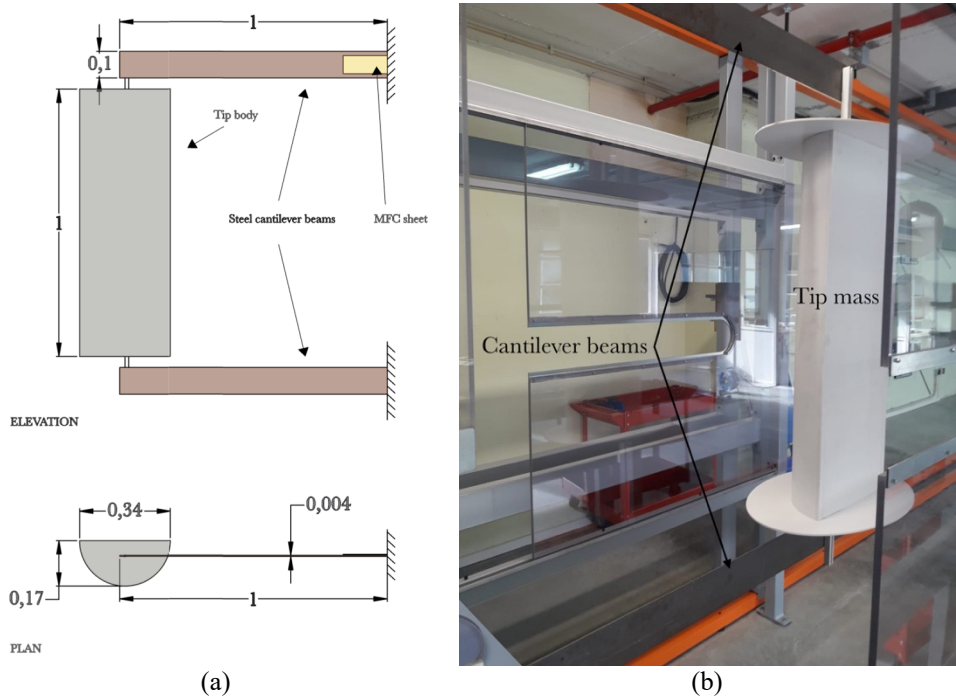

Figure 5:   Energy harvesting prototype. (a) Design scheme (dimensions in m); and
(b) Mounted in the test chamber.

Structural analyses have been carried out to guarantee the safe structural performance of the prototype and obtain dynamical properties (mass and natural frequencies) that would provide a strong dynamic response in the range of wind speeds attainable in the wind tunnel. In Table 2, the fundamental properties are reported. It must be noticed that the damping ratio of the prototype is one order of magnitude higher than the one of the sectional model, which may decrease the amplitude in the responses and prevent the interaction between VIV and galloping responses.

Table 2: Energy harvester prototype properties.

Property	Value
Natural frequency	1.56 Hz
Damping ratio	0.011
Mass	5.63 kg

A power output measurement circuit has been developed as well, based on an Arduino ONE board that reads the voltage output of the MFC sheet.

5 PROTOTYPE WIND TUNNEL TESTS

5.1 Wind-induced oscillations

The prototype, whose fundamental properties were introduced in the previous section, is tested in the wind tunnel for growing laminar wind flow velocities. The oscillations are measured and recorded using two accelerometers, one located at mid-span in the cantilever beam (Position 1 in the charts that are presented latter) and the other at the tip, where the amplitude of oscillation is maximum (Position 2). Additionally, the voltage output generated by the MFC sheet is recorded using the Arduino ONE board connected to a PC, previously described. It should be noticed that the semi-circular cylinder is rigidly connected at the tip of the cantilever beam, hence the oscillations are taking place in the first lateral natural mode of the system, and no coupling between plunge and torsional degrees of freedom is taking place, as it happened in the preliminary wind tunnel tests reported in Section 3.

In Fig. 6, the non-dimensional amplitude of oscillation measured at Positions 1 and 2 is plotted against the reduced wind flow speed. For comparison, the amplitudes of oscillation obtained in the preliminary wind tunnel tests are also provided, finding a good agreement in the reduced velocity regions showing significant excitation. This fact, justifies the feasibility of sectional model tests in the preliminary design of energy harvesters.

According to the wind tunnel tests, the prototype shows a narrow region of high oscillations for reduced velocities between 3 and 6, associated with VIV excitation. For reduced velocities higher than 15, the amplitude of oscillation steadily increases, which is a phenomenon associated to the built-up of galloping oscillations. It is therefore found that the harvester may be able to provide a significe energy output for two intervals in the reduced velocity, up to the maximum value of reduced velocity considered in the tests, which is 32.

5.2 Voltage output

During the experiment the voltage output of the MFC sheet has been recorded, obtaining a sinusoidal wave for each sampled wind velocity. In Fig. 7, the RMS values obtained for the range of studied wind speeds are reported. The time history of voltage output obtained for a
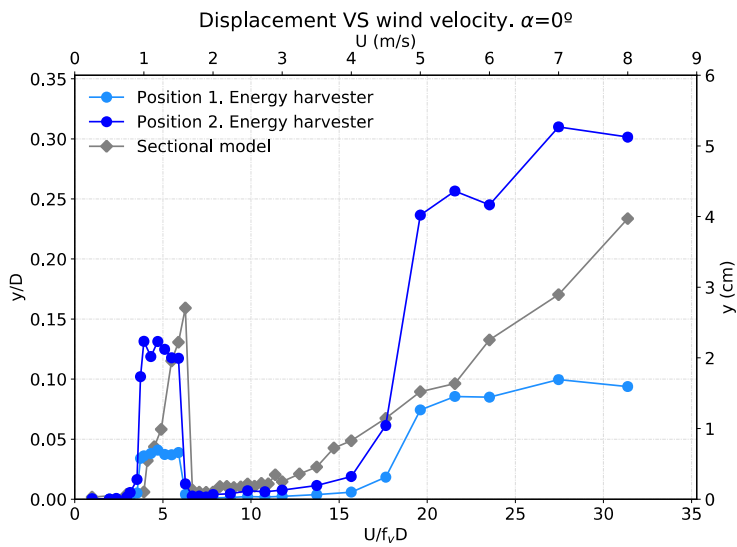
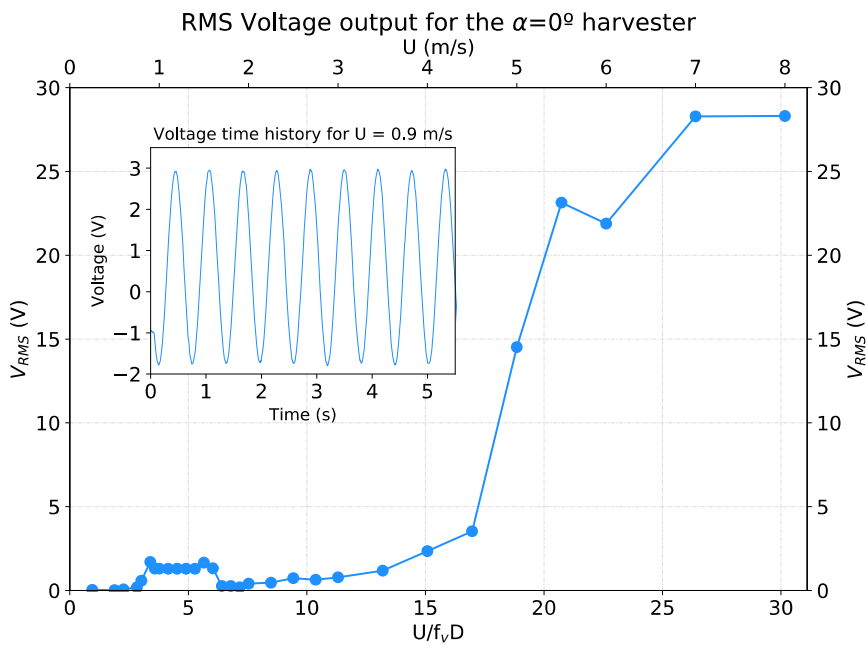Figure 6: Energy harvesting prototype oscillation response vs wind speed.

Figure 7: Voltage RMS vs wind speed curve.

low speed of 0.9 m/s that belongs to the lock-in region in the amplitude–velocity curve is also provided in Fig. 7.

5.3 Power output

The average harvested power obtained for the prototype at the 0° angle of attack configuration, for different values of the flow speed is reported in Fig. 8. The average power is evaluated as

$$P_{avg} = \frac{V_{RMS}^2}{R},$$

(5)

where R is the electrical resistance and V_{RMS} is the root mean square value of the voltage time history for a given flow speed.
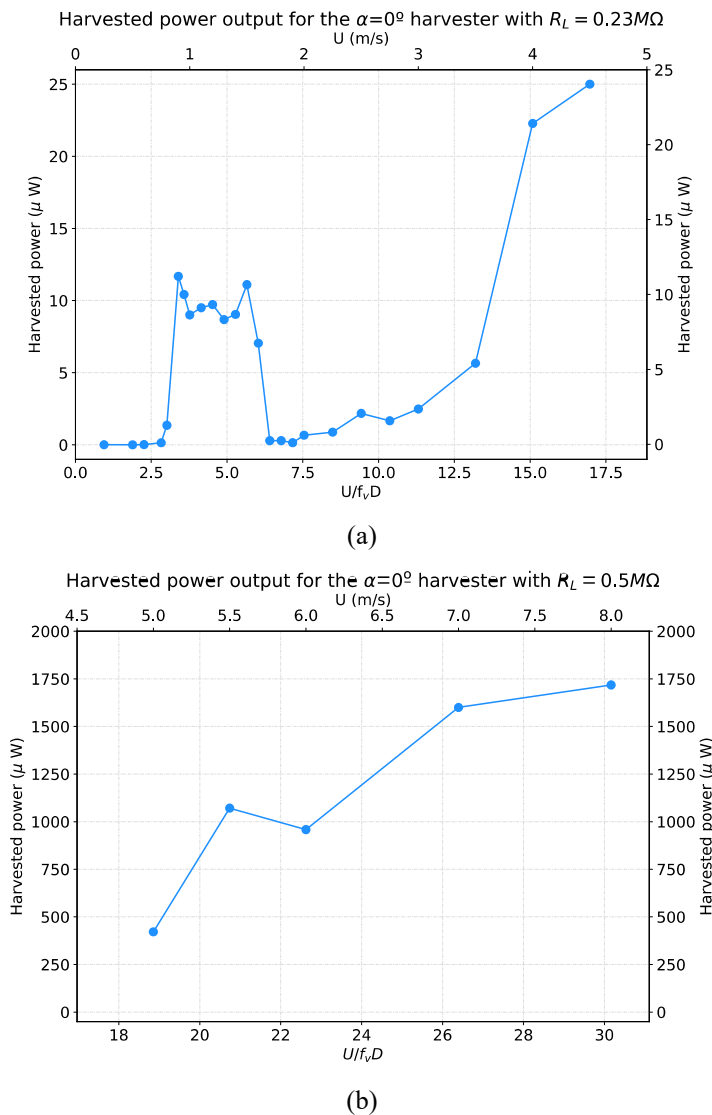

(a)

(b)

Figure 8:   Average harvested power vs wind speed. (a) U ≤ 4.5 m/s (R = 0.23 MΩ); and (b) U > 4.5 m/s (R = 0.5 MΩ).

In the tests, two different values of electrical resistance have been used. In the range of wind speeds lower than 4.5 m/s, $R = 0.23$ MΩ, while for U > 4.5 m/s, $R = 0.5$ MΩ.

In Fig. 8(a), it can be appreciated how at the VIV region the maximum average power output is about 12 μW; however, for higher wind speeds, at the incipient galloping condition, the average power output reaches up to 1700 μW, as it can be appreciated in Fig. 8(b) for a wind speed of 8 m/s. It should be noticed that a sensitivity study about the most feasible values of the electrical resistance to maximize the power output has not been carried out.

6 CONCLUSIONS AND FUTURE WORK

In this work a prototype for harvesting electrical energy from wind-induced oscillations of a bluff body has been introduced and its performance studied experimentally for smooth flow at 0° angle of attack.

A preliminary wind tunnel campaign of a sectional model of a semi-circular cylinder has allowed to identify the main aeroelastic phenomena that would be taking place at the studied range of flow speeds. Both VIV and coupled galloping phenomena were identified at different ranges of reduced velocities. Interestingly, a VIV-galloping interference case was identified for the torsional degree of freedom.

For the prototype, both VIV and galloping at the plunge degree of freedom were identified and the voltage and mean power output where recorded. This has showed the potential of the studied geometry to be used in the design of energy harvesters based on wind-induced oscillations.

This somehow preliminary study, while it has shown the feasibility of the prototype design for power generation, it has also opened the door for future studies. Among them, the following are highlighted: introduce subtle modifications in the studied geometry that might improve the prototype's performance, study different wind angles of attack that may show very different aeroelastic performance, and analyse the impact in the electrical generation performance of levels of turbulence in the incoming flow similar to those in natural wind.

REFERENCES

[1]   Elvin, N. & Erturk, A., Introduction and methods of mechanical energy harvesting. *Advances in Energy Harvesting Methods*, eds N. Elvin & A. Erturk, Springer, pp. 3–4, 2013.

[2]   Cid Montoya, M., Nieto, F., Alvarez, A.J., Hernández, S., Jurado, J.A. & Sánchez, R., Numerical simulations of the aerodynamic response of circular segments with different corner angles by means of 2D URANS: Impact of turbulence modeling approaches. *Engineering Applications of Computational Fluid Mechanics*, **12**(1), pp. 750–779, 2018.

[3]   Hu, G., Tse, K.T. & Kwok, K., Enhanced performance of wind energy harvester by aerodynamic treatment of a square prism. *Applied Physics Letters*, **108**, p. 123901, 2016.

[4]   Hu, G., Tse, K.T., Kwok, K., Jie, S. & Lyu, Y., Aerodynamic modification to a circular cylinder to enhance the piezoelectric wind energy harvesting. *Applied Physics Letters*, **109**, p. 193902, 2016.

[5]   Blevins, R.D., *Flow-Induced Vibration*, Krieger Publishing: Malabar, Florida, p. 43, p. 104, 1990.

[6] Naudascher, E. & Rockwell, D., *Flow-Induced Vibrations: An Engineering Guide*, A.A. Balkema: Rotterdam, Brookfield, pp. 188–189, 1994.

[7] Mannini, C., Marra, A.M., Massai, T. & Bartoli, G., Interference of vortex-induced vibration and transverse galloping for a rectangular cylinder. *Journal of Fluids and Structures*, **66**, pp. 403–423, 2016.